VAPOR—GAS FRONT IN THE CONDENSER OF A TWO-DIMENSIONAL GAS-CONTROLLED HEAT PIPE

V. V. Galaktionov, A. A. Parfent'eva,
D. V. Portnov, and V. Ya. Sasin

UDC 536.58

This paper describes a mathematical model for the flow of vapor in the condenser of a planar gas-controlled heat pipe (GCHP).

In the development and construction of gas-controlled heat pipes (GCHP) one needs to know the location and shape of the vapor—gas interface, which appreciably affects the operating conditions of the heat pipe and the length of the condensation zone. A number of papers have been published dealing with analytical and experimental investigation of heat and mass transfer in the region of the vapor—gas front (VGF) [1-6]. However, the literature does not give any velocity profiles in the vapor—gas front region of the GCHP. The present authors believe that the absence of velocity profiles stems from the complexity of the mathematical description of processes in the GCHP and the subsequent need to introduce a number of assumptions which do not always reflect the real physical picture.

For example, Samogyi and Yen [2], and also Rohani and Tien [3], give a two-dimensional analysis of the boundary zone between the gas and the vapor, based on the diffusion model of the VGF. Using the Kármán—Polhausen method of solution, Samogyi and Yen hypothesized that the vapor flow at the vapor—gas interface obeys a Hagen—Poiseuille law, which does not correspond with the real picture.

In the present work we propose that in the VGF region the basic mechanism for mass transfer is convective flow of vapor, causing the interface to be eroded. One can neglect the diffusion (i.e., molecular) component of transport compared with the convective. In addition, reverse flow of vapor can occur in the VGF region. To confirm the existence of these flows it is enough to obtain velocity profiles with reverse flows at the inlet to the vapor—gas region.

To solve this problem we use the momentum conservation equation

$$\tilde{U}\frac{\partial\tilde{U}}{\partial\tilde{X}}+\tilde{V}\frac{\partial\tilde{U}}{\partial\tilde{Y}}=-\frac{1}{\rho}\frac{\partial\tilde{P}}{\partial\tilde{X}}+\nu\left(\frac{\partial^2\tilde{U}}{\partial\tilde{X}^2}+\frac{\partial^2\tilde{U}}{\partial Y^2}\right) \tag{1}$$

and the mass conservation equation

$$\frac{\partial\tilde{U}}{\partial\tilde{X}}+\frac{\partial\tilde{V}}{\partial\tilde{Y}}=0. \tag{2}$$

In integral form with ρ = const we can write Eq. (2) in the form

$$\int_0^b\tilde{U}d\tilde{Y}=V_0(l_c-\tilde{X}). \tag{2'}$$

We transform Eqs. (1) and (2) by introducing the dimensionless variables U, V, Y, X:

$$\tilde{U}=\tilde{V}_0U;\quad\tilde{V}=\tilde{V}_0V\frac{b}{l_c};\quad\tilde{Y}=Yb;\quad\tilde{X}=Xl_c; \tag{3}$$

Moscow Power Institute. Translated from Inzhenerno-Fizicheskii Zhurnal, Vol. 42, No. 3, pp. 387-392, March, 1982. Original article submitted November 4, 1980.

0022-0841/82/4203-0273$07.50

$$U\frac{\partial U}{\partial X}+V\frac{\partial U}{\partial Y}=-\frac{\partial P}{\partial X}+\frac{1}{\mathrm{Re}_r}\left(\frac{1}{B}\frac{\partial^2 U}{\partial X^2}+B\frac{\partial^2 U}{\partial Y^2}\right); \tag{4}$$

$$\int_0^1 U\,dY=B(1-X), \tag{5}$$

where $P=\tilde{P}/\rho V_0^2$; $\mathrm{Re}_r=bV_0/\nu$; $B=l_c/b$.

Using the boundary condition at the permeable wall ($U=0$, $V=V_0$ at $Y=1$), and taking into account that $\partial P/\partial Y$ is negligibly small, we obtain

$$-\frac{\partial P}{\partial X}=V_0\left(\frac{\partial U}{\partial Y}\right)_{Y=1}-\frac{1}{\mathrm{Re}_r}\left(\frac{1}{B}\frac{\partial^2 U}{\partial X^2}+B\frac{\partial^2 U}{\partial Y^2}\right)_{Y=1}. \tag{6}$$

Allowing for Eq. (6), Eq. (4) takes the form

$$U\frac{\partial U}{\partial X}+V\frac{\partial U}{\partial Y}=V_0\left(\frac{\partial U}{\partial Y}\right)_{Y=1}-\frac{1}{\mathrm{Re}_r}\left(\frac{1}{B}\frac{\partial^2 U}{\partial X^2}+B\frac{\partial^2 U}{\partial Y^2}\right)_{Y=1}+\frac{1}{\mathrm{Re}_r}\left(\frac{1}{B}\frac{\partial^2 U}{\partial X^2}+B\frac{\partial^2 U}{\partial Y^2}\right), \tag{4'}$$

where, according to condition (3), $V_0=B$.

The axial velocity profile is approximated by a fourth-degree polynomial:

$$U=U_{00}[a(X)+b(X)Y^2+c(X)Y^4], \tag{7}$$

where $a(X)$, $b(X)$, $c(X)$ are coefficients, functions of X only, and X is the distance from the inlet to the condenser.

Using the Kármán–Polhausen integral relation, we transform Eq. (4) to the form

$$\frac{\partial}{\partial X}\int_0^1 U^2dY=B\left(1+\frac{1}{\mathrm{Re}_r}\right)\left(\frac{\partial U}{\partial Y}\right)_{Y=1}+\frac{1}{\mathrm{Re}_rB}\int_0^1\frac{\partial^2 U}{\partial X^2}dY-\frac{1}{\mathrm{Re}_r}\left(\frac{1}{B}\frac{\partial^2 U}{\partial X^2}+B\frac{\partial^2 U}{\partial Y^2}\right)_{Y=1}. \tag{8}$$

From Eqs. (7), (5), and (8) and the no-slip condition at the wall, $U=0$ (at $Y=1$), we obtain a system of three equations for the coefficients $a(X)$, $b(X)$, $c(X)$:

$$U_{00}\frac{\partial}{\partial X}\left[a^2(X)+\frac{b^2(X)}{5}+\frac{c^2(X)}{9}+\frac{2a(X)b(X)}{3}+\frac{2b(X)c(X)}{7}+\frac{2a(X)c(X)}{5}\right]=2B\left(1+\frac{1}{\mathrm{Re}_r}\right)\times$$

$$\times(b(X)+2c(X))-2B\frac{1}{\mathrm{Re}_r}(b(X)+6c(X));$$

$$U_{00}\left[a(X)+\frac{b(X)}{3}+\frac{c(X)}{5}\right]=B(1-X); \tag{9}$$

$$a(X)+b(X)+c(X)=0.$$

The differential equation in Eq. (9) is an equation of first order, and can be reduced [5] to a homogeneous differential equation. By simultaneous solution of the system of equations (9) we obtain

$$\left[\frac{2a(X)-[(\alpha-B^*)+\sqrt{4A+(\alpha-B^*)^2}](1-X)}{2a(X)-[(\alpha-B^*)-\sqrt{4A+(\alpha-B^*)^2}](1-X)}\right]^n=$$

$$=C'[A(1-X^2)+a(X)(\alpha-B^*)(1-X)-a^2(X)], \tag{10}$$

where

$$C'=\frac{1}{A+\alpha-B^*-1}\left[\frac{2-\alpha+B^*-\sqrt{4A+(\alpha-B^*)^2}}{2-\alpha+B^*+\sqrt{4A+(\alpha-B^*)^2}}\right];$$

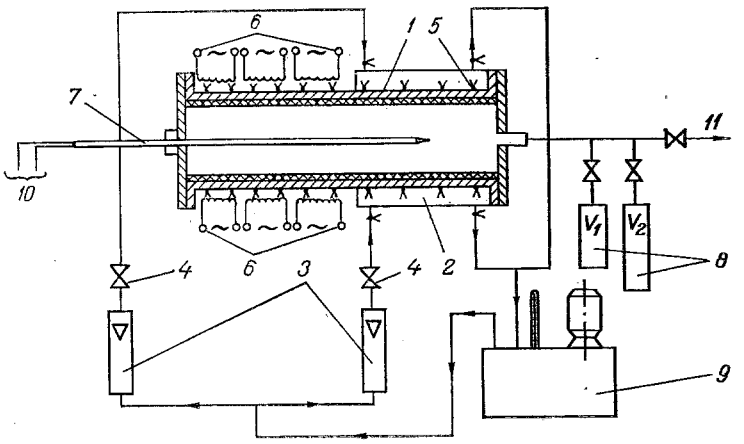

Fig. 1. Schematic diagram of the experimental equipment: 1) heat pipe body; 2) heat exchanger; 3) type RS-3A rotameter; 4) valves; 5) Chromel–Copel thermocouples; 6) three-segment electrical heater; 7) thermocouple probe; 8) reservoirs for gas; 9) thermostat; 10) outlet to the measuring instrument; 11) outlet to the atmosphere.

$$n = \frac{\alpha + B^*}{\sqrt{4A + (\alpha - B^*)^2}}; \quad \alpha = 0.94\,\frac{B}{U_{00}};$$

$$A = -6.15\left(\frac{B}{U_{00}}\right)^2 (12/\mathrm{Re}_r - 2.43); \quad B^* = \left(8.91 - \frac{49.22}{\mathrm{Re}_r}\right)\frac{B}{U_{00}}.$$

For the coefficients b(X) and c(X) we have:

$$b(X) = 7.5\frac{B}{U_{00}}(1 - X) - 6a(X); \tag{11}$$

$$c(X) = -[a(X) + b(X)]. \tag{12}$$

We used the ES-1022 computer to calculate the coefficients $a(X)$, b(X), c(X) and the velocity profiles U(X, Y) in the range of Re_r number from 0.001 to 4.18 or $0 \leqslant X < 1$ and for two values of the geometric parameter B = 10 and 20.

The Kármán–Polhausen method is approximate and is valid mainly for flows of boundary layer type. Nevertheless, the solution has shown that at the entrance to the VGF there is reverse flow of vapor, causing the observed erosion of the VGF. The extent of the reverse flow zone increases with increase of Re_r. For the flow examined in a planar channel the beginning of the reverse flow was set at the end of the section, at $X > 0.9$ for $\mathrm{Re}_r = 1$. The section where reverse flow began moved to the condenser inlet with increase of Re_r. For example, for $\mathrm{Re}_r = 4.18$, $X_B = 0.5$, i.e., it is located at the middle of the condenser.

For visual investigation of the VGF and of the influence of the various parameters on the shape and dimensions of the VGF we made up a planar GCHP and conducted an experimental investigation of its characteristics on the facility shown schematically in Fig. 1. The length of the GCHP is L = 430 mm, the side walls of the condenser and the evaporator have windows of size 178 × 17 mm, closed by quartz glass. The capillary-porous structure used is stainless steel mesh, and water is the heat transfer agent. Heat is supplied by a three-segment electrical heater, mounted on the top and bottom walls of the evaporator. The condenser is cooled by water with a constant inlet temperature. Chromel–Copel thermocouples are welded to the outside surface of the top and bottom walls of the GCHP. A thermocouple probe was used to measure the temperature inside the vapor space. The experiments were conducted with a initial pressure of P = 1 atm, and the condenser was open to the surroundings, i.e., $V_g = \infty$.

Smoke was injected through special apertures into the vapor volume from the evaporator side to visualize processes in the GCHP. The viewing windows were kept dry by superposed heaters. Pictures were taken during the visual observation of processes in the GCHP. The

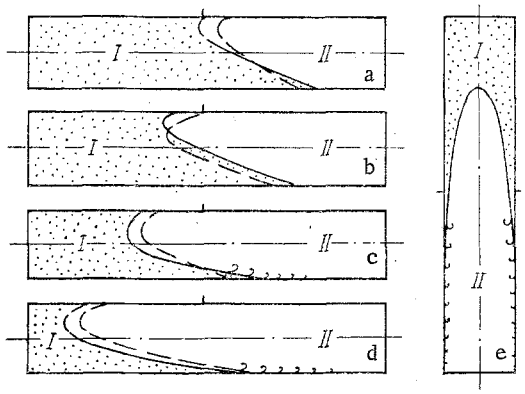

Fig. 2. Shape and position of the vapor–gas interface with variation in the heat load and arrangement of the GCHP: a) Q_f = 90 W; b) 125; c) 155; d) 190; e) 190; I) evaporator; II) condenser.

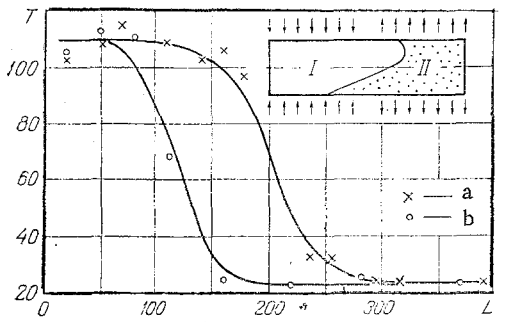

Fig. 3. Temperature distribution over the top (a) and bottom (b) walls of the heat pipe with q_e = 1.14 W/cm^2, $V_g = \infty$ and the shape of the VGF: I) evaporator; II) condenser. T is in °C and L is in mm.

model was tested both in a horizontal and in a vertical position. Typical shapes of the VGF are shown in Fig. 2, from the data of visual observations and photographs. It was established that the position of the vapor–gas interface depends on the power supplied, while the orientation of the GCHP in space influences the shape and erosion of the boundary. The latter effect is associated with the substantial difference of specific weight between water vapor and air. With the heat pipe horizontal, the vapor, being lighter, shifts to the upper part of the condensation zone of the GCHP, and the VGF shows a well-pronounced asymmetry. Figure 3 shows the shape of the VGF obtained from the visual observations, and temperature distribution curves over the top and bottom walls of the pipe. There is air at the lower wall over the whole length of the condenser, leading to a sharp drop in wall temperature. On the top wall a noticeable reduction in temperature is observed even in the condenser. At the end of the condenser the wall temperatures are the same.

With the help of the thermocouple probe we used the facility to determine the temperature profiles inside the GCHP. Figure 4 shows the temperature distribution for Q_f = 105 W. As can be seen from Fig. 4, one observes a rather extensive vapor region in which the temperature varies from close to the T_s of the vapor to the temperature of the surrounding air. The extent of this zone for Q = 105 W and $V_T = \infty$ is ∿7 cm. For low levels of power transferred by the heat pipe natural convection has an appreciable influence on erosion of the VGF. As a result the gas mixture is blown strongly towards the passive zone of the condenser, the erosion of the vapor front is reduced, and therefore, the transition region is contracted.

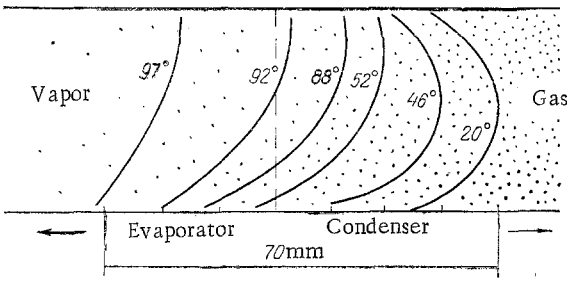

Fig. 4. Distribution of vapor temperature along the GCHP with Q_f = 105 W.

On the basis of the analytical, experimental, and visual investigations we have discovered the existence of reverse flows in the VGF region. The VGF has an appreciably asymmetric shape. The asymmetry, the instability, and the presence of vortices at the walls at the vapor–gas boundary confirms the hypothesis that the radial Reynolds number (Re_r), and the power supplied, appreciably affect the shape and form of the interface.

NOTATION

U, V, axial and radial components of the vapor velocity; X, Y, axial and radial coordinates; P, pressure; ρ, density; ν, kinematic viscosity; b, channel width; l_c, active length of the condenser; Re_r, radial Reynolds number; V_0, pumping speed at the wall; B, geometrical parameter; $a(X)$, b(X), c(X), coefficients; n, exponent; U_{oo}, dimensionless velocity on the axis at the condenser inlet; A, B*, α, groups depending on B, U_{oo}, and Re_r; q_e, specific heat flux in the evaporator; Q_f, total heat flux supplied to the evaporator.

LITERATURE CITED

1. D. K. Edwards and B. D. Marcus, "Heat and mass transfer in the vicinity of the vapor front in heat pipes," Trans. ASME, Ser. C, Teploperedacha, 94, No. 2, 31 (1972).
2. D. Somogyi and H. H. Yen, "An approximate analysis of the diffusing flow in a self-controlled heat pipe," J. Heat Transfer, 93 (1973).
3. A. R. Rohani and C. L. Tien, "Steady-state heat and mass transfer in the vapor–gas region of a heat pipe filled with noncondensible gas (two-dimensional approximation)," Trans. ASME Ser. C, Teploperedacha, 95, No. 3, 92 (1973).
4. S. Shimoji, H. Kimura, and T. Matsushita, "Prediction of evaporator temperature of a gas-loaded heat pipe by the diffuse front model," 3rd Int. Heat Pipe Conf., Palo Alto, Calif., May 1978, p. 155 (1978).
5. E. Kamke, Handbook of Ordinary Differential Equations [in German], Chelsea Publ.
6. Ooijen and C. I. Hoogendoorn, "Numerical calculations on the vapor flow in a flat plate heat pipe with asymmetrical boundary conditions," 3rd Int. Heat Pipe Conf., Palo Alto, Calif. (1978), p. 27.